

1 **REV-ERB Agonism Improves Liver Pathology in a Mouse**  
2 **Model of NASH**

3

4

5

6 Kristine Griffett\*, Gonzalo Bedia-Diaz, Bahaa Elgendy, and Thomas P. Burris

7

8

9

10

11

12

13

14

Center for Clinical Pharmacology, Washington University School of Medicine and St. Louis College of  
Pharmacy, St. Louis, MO

15

16

17

18

19

20

21

22

23

24

\*Corresponding Author

25

E-mail: [kgriffett@wustl.edu](mailto:kgriffett@wustl.edu)

## 26 **Abstract**

27 Non-alcoholic fatty liver disease (NAFLD) affects a significant number of people worldwide and  
28 currently there are no pharmacological treatments. NAFLD often presents with obesity, insulin  
29 resistance, and in some cases cardiovascular diseases. There is a clear need for treatment options to  
30 alleviate this disease since it often progresses to much more the much more severe non-alcoholic  
31 steatohepatitis (NASH). The REV-ERB nuclear receptor is a transcriptional repressor that regulates  
32 physiological processes involved in the development of NAFLD including lipogenesis and inflammation.  
33 We hypothesized that pharmacologically activating REV-ERB would suppress the progression of fatty  
34 liver in a mouse model of NASH. Using REV-ERB agonist SR9009 in a mouse NASH model, we  
35 demonstrate the beneficial effects of REV-ERB activation that led to an overall improvement of hepatic  
36 health by suppressing hepatic fibrosis and inflammatory response.

37

## 38 **Introduction**

39 Among the metabolic disorders, non-alcoholic fatty liver disease (NAFLD) is considered a hepatic  
40 manifestation of metabolic syndrome (MetS) and it is one of the prominent health challenges of the  
41 twenty-first century as NAFLD is the most prevalent liver disease worldwide affecting 25-30% of the  
42 general population and its prevalence could reach 70-90% in specific populations with comorbidities  
43 such as morbid obesity or type 2 diabetes mellitus [1-2]. NAFLD can often progress to non-alcoholic  
44 steatohepatitis (NASH), which is associated with progressive liver disease [1]. NASH has been mainly  
45 associated with higher morbidity and mortality than other diseases in the NAFLD spectrum and, although  
46 there are pharmacological therapies under clinical investigation for treatment of NASH [2], no drugs are  
47 approved by the Federal Drug Administration (FDA) or the European Medicines Agency (EMA) for the  
48 NASH treatment [3].

49 Nuclear receptors (NRs) are transcription factors generally activated by ligands and involved in  
50 diverse biological processes such as cell growth and differentiation, apoptosis, gene expression during

51 tumor formation and metabolism. They bind to specific sequences of DNA allowing them to regulate  
52 the expression of adjacent genes. Many diseases including NASH are directly or indirectly related to  
53 nuclear receptor signaling and many NRs have become favored targets for drug discovery [4]. NRs play  
54 an important role in liver diseases and they are key modulators in the onset and progression NAFLD,  
55 including the peroxisome proliferator-activated receptors (PPAR)  $\alpha/\beta/\gamma$ ; liver X receptors (LXR)  $\alpha/\beta$ ;  
56 farnesoid X receptors (FXR); constitutive androstane receptor (CAR); and pregnane X receptor (PXR).  
57 All of these NRs form obligate heterodimers with retinoid X receptor (RXR)  $\alpha/\beta/\gamma$  in order to modulate  
58 corresponding target genes in the nucleus [5,6].

59 REV-ERB nuclear receptors (REV-ERB $\alpha$  and REV-ERB $\beta$ ) are transcriptional repressors that  
60 regulate a variety of physiological processes including lipogenesis, inflammation, circadian regulation,  
61 and muscle regeneration and are expressed in all tissues but has significantly higher expression in liver,  
62 skeletal muscle, adipose tissue, and brain [7]. Although REV-ERBs play a regulatory role in hepatic  
63 metabolism, inflammation and lipogenesis, these NRs have yet to be validated as a potential therapeutic  
64 target for liver disease [8–11]. Here, we show that REV-ERB pan-agonist SR9009 treatment in *ob/ob*  
65 mice fed a high-fat, high-fructose (NASH) diet has beneficial effects and may provide some translational  
66 groundwork for further developing REV-ERB agonists for metabolic diseases, specifically NAFLD.

67

## 68 **Materials and Methods**

69

### 70 **Animals**

71 Animal studies were performed as previously described [12–14]. Briefly, six-week old B6 V-Lep<sup>ob/J</sup>  
72 (*ob/ob*) male mice were purchased from Jackson Labs (Bar Harbor, ME). Upon receipt, mice were housed  
73 individually in standard cages with huts and immediately placed on NASH diet (D09100301; Research  
74 Diets) [15]. Mice were maintained on this diet throughout the experiment. Mice were handled and  
75 weighed weekly while acclimating to the diet. At 12-weeks of age, mice were assigned into weight-  
76 matched groups (n = 7) and dosing began. Mice were weighed daily and food-intake was monitored

77 daily. At the termination of the study, mice were fasted and euthanized by CO<sub>2</sub> and blood was collected  
78 by cardiac puncture for clinical chemistry analysis at Scripps Florida Metabolism Core (Roche COBAS  
79 instrument) and ELISA analysis (EMD Millipore). Tissues were collected and flash-frozen in liquid  
80 nitrogen for gene expression, or placed in 4% Paraformaldehyde (PFA) in PBS for paraffin-embedding  
81 (Saint Louis University Histology Core) or 10% Neutral-Buffered Formalin (NBF) for cryo-sectioning.  
82 For intraperitoneal glucose tolerance test (ipGTT), mice were transferred to clean cages and fasted for  
83 12 hours overnight. Mice were weighed, baseline blood glucose was taken, then mice were given an  
84 injection of glucose solution in PBS (2g/kg body weight). Blood glucose levels were subsequently  
85 repeated at 30-, 60-, 90-, and 120-minutes following the injection of glucose. Mean blood glucose levels  
86 (mg/dL) are reported as well as the area under the curve (AUC) which was analyzed by two-tailed  
87 student's t-test in Graphpad prism. Following the ipGTT, mice were given access to food *ad libitum*.  
88 All animal work was approved by the Institutional Animal Care and Use Committee (IACUC) at  
89 Washington University in St. Louis (Protocol #20180062).

90

## 91 **Compounds and Dosing**

92 SR9009 was formulated as 100mg/kg at 10mg/ml in 5% DMSO, 15% Cremophore EL (Sigma), 80%  
93 PBS as previously described [16]. Both vehicle (5% DMSO, 15% CremophoreEL (Sigma), 80% PBS)  
94 and SR9009 were filter sterilized (Millipore Steriflip) prior to dosing. Mice were given once daily i.p.  
95 injections within an hour of "lights on" (ZT0-ZT1). Dosing was performed for 30 days by the same  
96 researcher.

97

## 98 **Gene Expression Analysis**

99 Total RNA was isolated from liver using the trizol (Invitrogen) method [12]. Samples were analyzed by  
100 QPCR using Fatty Liver and Fibrosis QPCR array plates (Bio-Rad; 384-well format) and Bio-Rad  
101 supplied SYBR reagents (per manufacturer's protocol). Each sample was run in duplicate and analyzed  
102 on the PrimePCR software supplied by Bio-Rad. Multiple reference genes were utilized (including

103 Gapdh, ActinB, and Cyclophilin) for analysis [14]. Results were plotted in GraphPad prism software as  
104 Gene Regulation using mean +/- SEM.

105

## 106 **Histology and Pathology Analysis**

107 Livers were placed in 4% PFA at 4°C overnight and then were paraffin-embedded and sectioned at 10  
108 µm onto slides at the Saint Louis University Histology Core Facility. H&E and Masson’s Trichrome  
109 staining were also performed at the core as a fee-for-service [12,14,17].. Stained sections (both H&E  
110 and Masson’s Trichrome) were sent to Reveal Biosciences (San Diego, CA) for quantification of fibrosis,  
111 inflammation, steatosis, hepatocellular ballooning, and presence of Mallory Bodies utilizing AI-based  
112 digital pathology and image processing. Briefly, whole slide images were generated using 3D Histech  
113 Panoramic SCAN and uploaded into imageDx™ software. Each scanned image was assessed for  
114 quality and accuracy, then machine learning algorithms were applied to perform automated image quality  
115 control assessments and quantitative measurements of disease features across the entire tissue. For  
116 steatosis analysis, lipid regions within the H&E slides were identified and quantitated as a percent of the  
117 total image analysis area. For hepatocyte ballooning, these hepatocytes were identified and quantitated  
118 as the number of ballooning cells within the total image analysis area of the H&E stained sections.  
119 Positive ballooning was identified based on cell diameter and presence of disrupted cytoskeletal  
120 structure. The number of ballooning cells was counted and expressed as density across the total area.  
121 Inflammatory cells were identified and quantitated on H&E slides as the number of immune cells within  
122 the total image analysis area. The number of immune cells was counted and measured as the immune  
123 cell density, total number, and area of immune cells. For fibrosis, collagen and extracellular matrix fibers  
124 were identified in the Masson’s Trichrome-stained slides and quantitated as a percent of the total image  
125 analysis area. H&E sections were also used to identify the presence of Mallory bodies within the total  
126 image analysis areas.

127

## 128 **Statistics**

129 All data are expressed as mean +/- SEM (n = 4 or greater). All expression statistical analysis was  
130 performed using ANOVA with Tukey's post-hoc analysis in GraphPad prism software. Weekly mouse  
131 weights and food intake data was analyzed by two-way ANOVA followed by Sidak's multiple  
132 comparisons at the 95% confidence level. For ipGTT, area under the curve (AUC) was generated and  
133 the data was analyzed by two-tailed student's t-test in GraphPad prism software. Sample data generated  
134 by Reveal Biosciences was entered into Graphpad prism software and analyzed for statistical significance  
135 using an unpaired student's t-test (2-tailed). P-values are reported as follows: \*  $p \leq 0.05$ , \*\*  $p \leq 0.01$ ,  
136 \*\*\*  $p \leq 0.001$ , and \*\*\*\*  $p \leq 0.0001$ .

137

## 138 **Results**

139 Given that REV-ERBs have been demonstrated to play a regulatory role in hepatic lipid  
140 metabolism [18] as well as inflammation [16,18,19], we sought to examine the effects of  
141 pharmacologically activating REV-ERB in a mouse model of NASH and determine whether REV-ERB  
142 may be a therapeutically relevant target. We opted to utilize a diet-induced NASH model using *ob/ob*  
143 mice as previously described [14,15] as the time period for development of NAFLD with fibrosis  
144 (NASH) is relatively short as compared to other models. During the acclimation and NASH development  
145 period, mice were fed a diet that contains Primex as a trans-fat source, fructose, and cholesterol *ad libitum*  
146 and monitored for weight gain and food intake. These parameters were also monitored daily throughout  
147 the dosing period to validate that any weight-loss was not due to loss of appetite. As shown in Figure 1A,  
148 both groups (Vehicle and SR9009) gained weight throughout the experimental period, however the  
149 SR9009-treated group gained weight at a consistently slower rate. The slower weight gain was not due  
150 to lower food intake in the SR9009-treated mice since this group consistently consumed the same amount  
151 of food as the vehicle group (Figure 1B). After 30-days of dosing was completed, mice were euthanized,  
152 and we performed a variety of tissue and plasma analyses to determine whether SR9009 treatment had a  
153 beneficial effect in this model. While we did not see a significant effect in liver weight as a percentage

154 of total body weight (S1 Fig), we did observe a decrease in the fat mass of the SR9009-treated animals,  
155 while lean mass was unchanged (Fig 1C). We were interested in determining whether SR9009 had any  
156 utility in improving the hepatic health of these mice. In order to make this determination, we performed  
157 clinical chemistry analysis on blood plasma samples to examine liver enzyme levels. ALT was  
158 significantly decreased in the SR9009-treated group (Fig 1D). While not statistically significant, AST  
159 levels in the SR9009 group were also trending lower than the vehicle group consistent with a benefit due  
160 to SR9009 treatment (S1 Fig). These data suggest that that the amount of liver damage due to the diet  
161 may be suppressed by treatment with REV-ERB agonist SR9009. In addition to effects on hepatic  
162 enzymes, we also observed a significant decrease in fasted blood-glucose levels in the SR9009-treated  
163 mice (Fig 1E). The *ob/ob* mouse model is typically hyperglycemic and addition of the high fat/high  
164 fructose diet hyperglycemia can be particularly prominent. During the third week of dosing, we  
165 performed an ipGTT on the mice (Fig 1F) and observed that while both groups of mice were  
166 hyperglycemic, the SR9009-treated group responded better to the bolus of glucose. In fact, the difference  
167 in AUC was statistically significant between the two groups (Fig 1F right panel) as analyzed by a two-  
168 tailed student's t-test ( $p = 0.027$ ), although final plasma insulin levels were not affected by the treatment  
169 (S1 Fig). Thus, our observation that of lowered hyperglycemia was promising and potentially relevant  
170 to human NASH patients who often present with co-morbidities such as obesity and diabetes [20–24].

171  
172 **Figure 1: REV-ERB agonist treatment of *ob/ob* NASH diet-fed mice.**

173 Mouse weight (A) and food intake (B) were recorded daily and averaged weekly for each group. At the  
174 termination of the experiment, mice were euthanized and blood and tissues were collected for analysis.  
175 Panel C shows body composition of lean and fat mass for each group. ALT (D), fasting blood glucose  
176 (E), ipGTT and area under curve (AUC) (F), circulating triglycerides (G), and circulating cholesterol  
177 levels (H) were also analyzed from blood plasma.

178  
179 Hyperlipidemia is also a comorbidity in NASH patients, therefore we also analyzed circulating  
180 triglyceride levels (Fig 1G) and total cholesterol levels (Fig 1H) in both mouse groups. We also observed  
181 significantly reduced total protein in the plasma of SR9009 mice as compared to vehicle-treated mice

182 (S1 Fig). Our overall impression from the clinical chemistry data and mouse observations is that SR9009  
183 treatment may have beneficial effects in a NASH model.

184 As the SR9009 group maintained a lower body weight throughout the dosing period and had  
185 significantly decreased circulating lipid levels in blood plasma, we investigated whether the SR9009-  
186 treated mice had reduced hepatosteatosis (both macrovesicular and microvesicular) [12,14,17]. Figure  
187 2A and 2B show the total lipid accumulation and percentage of tissue covered in lipid accumulation  
188 based on the H&E stained liver sections for both vehicle- and SR9009-treated animals. There is no  
189 change in either macrovesicular or microvesicular steatosis (S1 Table), suggesting that the beneficial  
190 effects observed in this mouse model may not be attributable to REV-ERB's role in reduced fat mass.

191  
192 **Figure 2: Hepatosteatosis in *ob/ob* mice maintained on a NASH diet does not appear affected in**  
193 **SR9009-treated group.**

194 Digital pathology analysis suggests that SR9009 treatment in NASH mice may not suppress total hepatic  
195 lipid area (A) or total percentage of lipids within the entire section (B). While steatosis appears  
196 unaffected by SR9009 treatment, the number of ballooning hepatocytes is decreased in the treated mice  
197 although the effect does not reach significance (C). (D) H&E sections of representative livers for vehicle  
198 (top) and SR9009 (bottom). Scale bar for vehicle section indicates 1.56 mm. Scale bar for SR9009  
199 section indicates 3.11 mm. For steatosis quantitation, macro droplet > 65  $\mu\text{m}^2$ ; micro droplet  $\leq$  65  $\mu\text{m}^2$ .

200  
201 To validate the clinical chemistry data suggesting that the SR9009 reduced liver damage and  
202 improved liver health, quantitated hepatocyte ballooning density from H&E stained liver sections. As  
203 shown by Fig 2C, SR9009-treated mice have a lowered density of hepatocyte ballooning as compared to  
204 vehicle-treated mice. While this was not statistically significant ( $p = 0.0903$ ), it suggests that treatment  
205 with SR9009 may have slowed the progression of NASH in these animals. We were intrigued that REV-  
206 ERB agonism in this model did not significantly affect steatosis in the liver with its known role in lipid  
207 metabolism, but appeared to suppress circulating cholesterol and reduce overall body fat mass. Therefore  
208 we assessed the expression levels of several known REV-ERB target genes involved in hyperlipidemia  
209 (*Dhcr24*, *ApoE*, and *ApoC3*) by QPCR and observed a significant decrease in these genes (S2 Fig)  
210 suggesting that SR9009 activation of REV-ERB is suppressing cholesterol and lipid metabolism but may  
211 not have efficacy in this model in which treatment started well after the development of NASH began.



212 While hepatic steatosis was not significantly affected by SR9009 treatment in this model, we  
213 further investigated clinical chemistry findings that SR9009 improves hepatic health by quantitating  
214 fibrosis and immune cell infiltration in liver sections (Fig 3A). We first evaluated the Masson's trichrome  
215 stained sections and identified the collagen and extracellular matrix fibers stained with deep blue within  
216 the whole slide image. Positive collagen fibers were then visualized using an overlaid green mask and  
217 measured as a percentage of the total image analysis area (S3 Fig). The calculated percent area of positive  
218 collagen (fibrosis) was significantly reduced in the SR9009-treated mice (Fig 3B) suggesting that the  
219 beneficial hepatic effects from REV-ERB agonism in this model may be due to suppressed fibrosis.  
220 Further analysis of H&E staining also indicated a reduced number of inflammatory foci and immune cell  
221 count, although these did not reach significance in our analysis (Fig 3C-D). Additionally, H&E sections  
222 indicated that all liver samples in this study showed the presence of Mallory Bodies, however the overall  
223 morphology of the SR9009-treated livers appeared improved as compared to the vehicle group (S1  
224 Table). Overall, these results suggest that SR9009 treatment halted the progression of NASH in this  
225 mouse model by reducing hepatic inflammation and suppressing fibrosis.

226

227 **Figure 3: SR9009 Significantly Reduced Fibrosis and Suppressed Inflammatory Activity.**

228 (A) Masson's Trichrome staining of liver sections (representative samples). Vehicle pictured at the top  
229 shows significant collagen formation. (B) Quantitated analysis of the Masson's Trichrome staining for  
230 fibrosis as measured by percent of the total area. Immune Cell Density (C) and Immune Cell Count (D)  
231 are unchanged, but appear to be less active as fibrosis is significantly reduced in SR9009 samples. Scale  
232 bars indicate 1.56 mm.

233

234 To continue our investigation into whether pharmacological activation of REV-ERB is beneficial  
235 in an NASH model, we analyzed gene expression of inflammatory markers by QPCR from frozen mouse  
236 liver tissues. For this analysis, we focused on expression changes related to inflammatory markers that  
237 indicate progression of NAFLD towards a NASH pathology, specifically *IL-1 $\alpha$* , *IL-1 $\beta$* , *Ifn $\gamma$* , and *TNF $\alpha$* .  
238 Previous work from our lab [16] and others have shown that REV-ERBs regulate a variety of genes  
239 involved in the pathogenesis of metabolic diseases including those associated with inflammation.  
240 Specifically, we were interested to see whether we were suppressing the progression of NAFLD towards

241 NASH with SR9009 by not only alleviating liver damage as assessed in Figure 1D-H, but by also  
242 suppressing hepatic inflammation in these animals, which was suggested in the H&E staining (Figure 2).  
243 Indeed, when compared to the vehicle-treated group, the SR9009 mice display significantly lower levels  
244 of expression of inflammatory cytokines, all of which have been implicated as biomarkers in NASH  
245 progression (Figure 4A). Since we observed a significant reduction in fibrosis in the SR9009-treated  
246 animals, we also assessed pro-fibrotic gene expression by QPCR. Fig 4B confirms that pharmacological  
247 activation of REV-ERB significantly reduces the expression of various pro-fibrotic genes including  
248 *Col3A1*, *Acta2*, *STAT1*, *Mmp13*, *Timp1*, and *TGF $\beta$*  [25]. Interestingly, several other pro-inflammatory  
249 genes (*Col1A2* and *Agt*) are not affected by SR9009 treatment suggesting that REV-ERB may play a role  
250 in the regulation of a select array pro-fibrotic genes involved in NASH progression. While these results  
251 indicated a significant effect on pro-inflammatory and pro-fibrotic genes in liver tissues, we sought to  
252 assess peripheral inflammation in these animals as well. We assessed plasma TNF $\alpha$  using levels at the  
253 time of euthanasia and as shown in Figure 4C, SR9009-treated mice display significantly reduced  
254 circulating TNF $\alpha$  levels. This suggests that activation of REV-ERB in a NASH model may dampen the  
255 progression of NAFLD towards NASH and improve hepatic health by suppressing fibrosis and  
256 inflammatory activity.

257  
258 **Figure 4: Expression of inflammatory markers are downregulated by SR9009 treatment in a mouse**  
259 **model of NASH.**

260 (A) Gene expression of inflammatory cytokines (*IL-1a*, *IL-1b*, *IFN $\gamma$* , *TNF $\alpha$* , and *NF $\kappa$ B*) in mouse liver  
261 tissues that are involved in the pathogenesis of NAFLD-NASH. (B) Gene expression was also performed  
262 for pro-fibrotic genes. As shown in the figure, several genes are significantly downregulated by SR9009  
263 pharmacological activation of REV-ERB. (C) An ELISA for mouse TNF $\alpha$  was performed using plasma  
264 samples from each mouse in triplicate and shows that SR9009 mice had significantly reduced circulating  
265 TNF $\alpha$ .

266

## 267 **Discussion**

268 Over the last several years, many studies by our lab and others have demonstrated that the REV-ERBs

269 regulate a variety of genes involved in lipogenesis, metabolism, and inflammation (Fig 5). Several studies  
270 have investigated potential of REV-ERB agonists as potential therapeutics for cardio-metabolic diseases  
271 including atherosclerosis which is a common comorbidity with NAFLD or NASH [16,19].  
272 Understanding the critical role that the REV-ERBs play in these pathways, we hypothesized that  
273 pharmacological activation of REV-ERB, with the tool compound SR9009, in a mouse model of NASH  
274 would provide beneficial metabolic effects in the liver leading to reduced NASH pathology. While the  
275 SR9009 group did not gain weight at the same rate as the vehicle group and we cannot validate whether  
276 this was a direct effect of the compound, although feeding and other behaviors were observed to be the  
277 same for both groups throughout the study. Our data clearly suggests that SR9009 improved the  
278 metabolic profile in the mice (reduced glucose levels and improved glucose tolerance) while also  
279 improving hepatic health by suppressing inflammation that essential for the progression of NAFLD to  
280 NASH. Most importantly, we observed a significant reduction in expression of pro-fibrotic genes in the  
281 liver, which was consistent with reduced hepatic fibrosis.

282 **Figure 5: The Nuclear Receptor REV-ERB Regulates Inflammation, Lipid Metabolism, and**  
283 **Glucose Metabolism by Recruiting NCoR to Suppress Transcriptional Activation of Target**  
284 **Genes.**

285 This schematic demonstrates how the REV-ERB nuclear receptors regulate transcription of target genes  
286 that are involved in inflammation, and lipid and glucose metabolism. Upon agonist binding to REV-  
287 ERB, a conformational change occurs and allows for the nuclear receptor co-repressor complex (NCoR)  
288 to bind and inhibit the transcription of target genes. As REV-ERBs are regulators of inflammation and  
289 hepatic metabolism, it was hypothesized that pharmacological activation of REV-ERB in a NASH model  
290 would improve overall hepatic health by suppressing genes involved in lipid metabolism. As indicated  
291 by the results, SR9009 actually had little to no effect on lipid metabolism but improved overall clinical  
292 indications of NASH in this model. Further investigation demonstrated that REV-ERB agonism in a  
293 NASH model suppresses hepatic inflammation and fibrosis and shows therapeutic benefit in dampening  
294 the progression of this disease. Image created in Biorender.

295

296 Interestingly, we did not observe a significant effect on hepatic steatosis or total lipid  
297 accumulation, suggesting that the beneficial effects of REV-ERB agonism in this model may not be due  
298 to REV-ERB's role in reduction of fat mass. Based on the quantitative analysis performed on the liver  
299 sections, it appears that hepatocyte ballooning was somewhat decreased in the SR9009 group, although

300 this did not reach significance. This study was performed in a fairly short period of time (30 days) and  
301 it is possible that an extended period of dosing may have a more beneficial effect on hepatic steatosis.  
302 We originally designed our hypothesis based on our previous study [18] that demonstrated a significant  
303 metabolic impact in hepatic lipogenesis and obesity in DIO mice. In this study, SR9009 was dosed twice  
304 per day (at 100 mg/kg) and resulted in significant repression of lipogenic and metabolic genes, as well  
305 as significant reduction in overall body weight. It is possible that in the current study, the once per day  
306 dosing (100 mg/kg) that was utilized to reduce animal stress did not reach the maximal potential efficacy  
307 in the NASH model. We utilized SR9009 as a tool to activate REV-ERB in vivo and currently there are  
308 limited pharmacological tools available, but in terms of a pharmacological agent SR9009 has relatively  
309 poor potency (1  $\mu$ M range), solubility, and pharmacokinetic properties that lead to a quick clearance time  
310 that may attribute to lowered efficacy. Novel REV-ERB compounds with improved potency and  
311 pharmacokinetic profiles may provide efficacy in NASH studies to suppress hepatic metabolic activity,  
312 inflammation, and fibrosis in the future.

313 In summary, our data suggests that REV-ERB is a potential therapeutic target to slow the  
314 progression of NAFLD towards NASH. The REV-ERB agonist SR9009 displayed efficacy in reduction  
315 of hepatic pathology associated with NASH. SR9009 is effective in suppressing clinical markers of liver  
316 damage, circulating lipids, hepatic fibrosis and markers of inflammation. Our data suggests that REV-  
317 ERB agonists may offer novel therapies for NAFLD or NASH in the future.

318

## 319 **Acknowledgments**

320 We thank Barb Nagel at Saint Louis University School of Medicine (St. Louis, MO) Histology Core for  
321 paraffin embedding and performing histological staining of liver sections, Melissa Kazantzis at The  
322 Scripps Research Institute in Jupiter, FL for performing clinical chemistry analysis on samples and  
323 Sherry Burris for sectioning of liver samples.

324

## 325 **References**

- 326 1. Fazel Y, B. Koenig A, Sayiner M, D. Goodman Z, M. Younossi Z. Epidemiology and natural  
327 history of non-alcoholic fatty liver disease [Internet]. *Metabolism*. 2016. pp. 1017 – 1025.  
328 doi:<https://doi.org/10.1016/j.metabol.2016.01.012>
- 329
- 330 2. Polyzos SA, Kang ES, Boutari C, Rhee E-J, Mantzoros CS. Current and emerging  
331 pharmacological options for the treatment of nonalcoholic steatohepatitis. *Metabolism*. Elsevier  
332 BV; 2020; 154203. doi:[10.1016/j.metabol.2020.154203](https://doi.org/10.1016/j.metabol.2020.154203)
- 333
- 334 3. Konerman MA, Jones JC, Harrison SA. Pharmacotherapy for NASH: Current and emerging.  
335 *Journal of Hepatology*. Elsevier BV; 2018;68: 362–375. doi:[10.1016/j.jhep.2017.10.015](https://doi.org/10.1016/j.jhep.2017.10.015)
- 336
- 337 4. Yang X, Gonzalez FJ, Huang M, Bi H. Nuclear receptors and non-alcoholic fatty liver disease:  
338 An update. *Liver Research*. Elsevier BV; 2020; doi:[10.1016/j.livres.2020.03.001](https://doi.org/10.1016/j.livres.2020.03.001)
- 339
- 340 5. Tanaka N, Aoyama T, Kimura S, Gonzalez FJ. Targeting nuclear receptors for the treatment of  
341 fatty liver disease. *Pharmacology & Therapeutics*. Elsevier BV; 2017;179: 142–157.  
342 doi:[10.1016/j.pharmthera.2017.05.011](https://doi.org/10.1016/j.pharmthera.2017.05.011)
- 343
- 344 6. López-Velázquez JA, Carrillo-Córdova LD, Chávez-Tapia NC, Uribe M, Méndez-Sánchez N.  
345 Nuclear Receptors in Nonalcoholic Fatty Liver Disease. *Journal of Lipids*. Hindawi Limited;  
346 2012;2012: 1–10. doi:[10.1155/2012/139875](https://doi.org/10.1155/2012/139875)
- 347
- 348 7. Preitner N, Damiola F, Luis-Lopez-Molina, Zakany J, Duboule D, Albrecht U, et al. The Orphan  
349 Nuclear Receptor REV-ERB $\alpha$  Controls Circadian Transcription within the Positive Limb of the  
350 Mammalian Circadian Oscillator. *Cell*. Elsevier BV; 2002;110: 251–260. doi:[10.1016/s0092-8674\(02\)00825-5](https://doi.org/10.1016/s0092-8674(02)00825-5)
- 351
- 352
- 353 8. Li T, Eheim AL, Klein S, Uschner FE, Smith AC, Brandon-Warner E, et al. Novel role of nuclear  
354 receptor rev-erb $\alpha$  in hepatic stellate cell activation: Potential therapeutic target for liver injury.  
355 *Hepatology*. Wiley; 2014;59: 2383–2396. doi:[10.1002/hep.27049](https://doi.org/10.1002/hep.27049)
- 356
- 357 9. Stujanna EN, Murakoshi N, Tajiri K, Xu D, Kimura T, Qin R, et al. Rev-erb agonist improves  
358 adverse cardiac remodeling and survival in myocardial infarction through an anti-inflammatory  
359 mechanism. Fan G-C, editor. *PLOS ONE*. Public Library of Science (PLOS); 2017;12: e0189330.  
360 doi:[10.1371/journal.pone.0189330](https://doi.org/10.1371/journal.pone.0189330)
- 361
- 362 10. Kojetin D.J. and Burris T.P. A Role for Rev-erb $\alpha$  Ligands in the Regulation of Adipogenesis.  
363 *Current Pharmaceutical Design*. Bentham Science Publishers Ltd.; 2011;17: 320–324.  
364 doi:[10.2174/138161211795164211](https://doi.org/10.2174/138161211795164211)
- 365
- 366 11. Pariollaud M, Gibbs JE, Hopwood TW, Brown S, Begley N, Vonslow R, et al. Circadian clock  
367 component REV-ERB $\alpha$  controls homeostatic regulation of pulmonary inflammation. *Journal of*  
368 *Clinical Investigation*. American Society for Clinical Investigation; 2018;128: 2281–2296.  
369 doi:[10.1172/jci93910](https://doi.org/10.1172/jci93910)
- 370

- 371 12. Griffett K, Solt LA, El-Gendy BE-DM, Kamenecka TM, Burris TP. A Liver-Selective LXR  
372 Inverse Agonist That Suppresses Hepatic Steatosis. *ACS Chemical Biology*. American Chemical  
373 Society (ACS); 2012;8: 559–567. doi:10.1021/cb300541g  
374
- 375 13. Griffett K, Burris TP. Promiscuous activity of the LXR antagonist GSK2033 in a mouse model  
376 of fatty liver disease. *Biochemical and Biophysical Research Communications*. Elsevier BV;  
377 2016;479: 424–428. doi:10.1016/j.bbrc.2016.09.036  
378
- 379 14. Griffett K, Welch RD, Flaveny CA, Kolar GR, Neuschwander-Tetri BA, Burris TP. The LXR  
380 inverse agonist SR9238 suppresses fibrosis in a model of non-alcoholic steatohepatitis. *Molecular*  
381 *Metabolism*. Elsevier BV; 2015;4: 353–357. doi:10.1016/j.molmet.2015.01.009  
382
- 383 15. Trevaskis JL, Griffin PS, Wittmer C, Neuschwander-Tetri BA, Brunt EM, Dolman CS, et al.  
384 Glucagon-like peptide-1 receptor agonism improves metabolic, biochemical, and  
385 histopathological indices of nonalcoholic steatohepatitis in mice [Internet]. *American Journal of*  
386 *Physiology-Gastrointestinal and Liver Physiology*. 2012. pp. G762–G772.  
387 doi:10.1152/ajpgi.00476.2011  
388
- 389 16. Sitaula S, Billon C, Kamenecka TM, Solt LA, Burris TP. Suppression of atherosclerosis by  
390 synthetic REV-ERB agonist. *Biochemical and Biophysical Research Communications*. Elsevier  
391 BV; 2015;460: 566–571. doi:10.1016/j.bbrc.2015.03.070  
392
- 393 17. Sengupta M, Griffett K, Flaveny CA, Burris TP. Inhibition of Hepatotoxicity by a LXR Inverse  
394 Agonist in a Model of Alcoholic Liver Disease. *ACS Pharmacology & Translational Science*.  
395 American Chemical Society (ACS); 2018;1: 50–60. doi:10.1021/acscptsci.8b00003  
396
- 397 18. Solt LA, Wang Y, Banerjee S, Hughes T, Kojetin DJ, Lundasen T, et al. Regulation of circadian  
398 behaviour and metabolism by synthetic REV-ERB agonists. *Nature*. Springer Science and  
399 Business Media LLC; 2012;485: 62–68. doi:10.1038/nature11030  
400
- 401 19. Pourcet B, Zecchin M, Ferri L, Beauchamp J, Sitaula S, Billon C, et al. Nuclear Receptor  
402 Subfamily 1 Group D Member 1 Regulates Circadian Activity of NLRP3 Inflammasome to  
403 Reduce the Severity of Fulminant Hepatitis in Mice. *Gastroenterology*. Elsevier BV; 2018;154:  
404 1449–1464.e20. doi:10.1053/j.gastro.2017.12.019  
405
- 406 20. Petit J-M, Vergès B. GLP-1 receptor agonists in NAFLD. *Diabetes & Metabolism*. Elsevier BV;  
407 2017;43: 2S28–2S33. doi:10.1016/s1262-3636(17)30070-8  
408
- 409 21. Scorletti E, Byrne CD. Extrahepatic Diseases and NAFLD: The Triangular Relationship between  
410 NAFLD, Type 2-Diabetes and Dysbiosis. *Digestive Diseases*. S. Karger AG; 2016;34: 11–18.  
411 doi:10.1159/000447276  
412
- 413 22. Obesity, Type 2 diabetes and NAFLD. *Diabetic Medicine*. Wiley; 2014;31: 1–3.  
414 doi:10.1111/dme.12377\_1  
415
- 416 23. Portillo-Sanchez P, Cusi K. Treatment of Nonalcoholic Fatty Liver Disease (NAFLD) in patients  
417 with Type 2 Diabetes Mellitus. *Clinical Diabetes and Endocrinology*. Springer Science and  
418 Business Media LLC; 2016;2. doi:10.1186/s40842-016-0027-7  
419

- 420 24. Bonora E. Novel predictors of diabetes - NAFLD, diabetes and CVD. *Endocrine Abstracts*.  
421 *Bioscientifica*; 2017; doi:10.1530/endoabs.49.s29.3  
422
- 423 25. Feng G, Li X-P, Niu C-Y, Liu M-L, Yan Q, Fan L-P, et al. Bioinformatics analysis reveals novel  
424 core genes associated with nonalcoholic fatty liver disease and nonalcoholic steatohepatitis  
425 [Internet]. *Gene*. 2020. p. 144549. doi:<https://doi.org/10.1016/j.gene.2020.144549>  
426  
427

## 428 **Supporting Information**

429

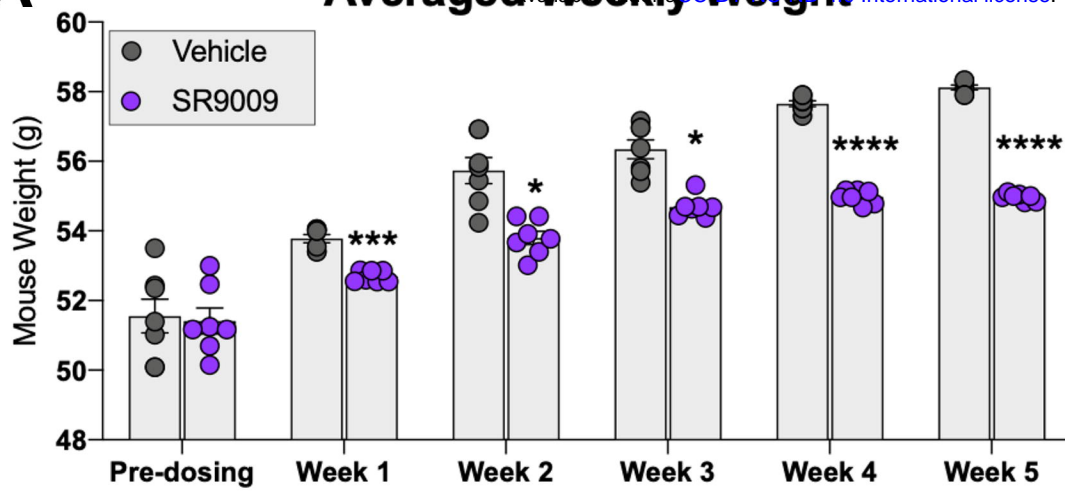
430 **S1 Fig. Additional clinical chemistry analysis of plasma from mouse NASH model.** Percentage of  
431 Liver weight to total body weight, AST levels, and plasma insulin levels were not significantly changed  
432 by SR9009 treatment although total protein was significantly reduced in these mice.  
433

434 **S2 Fig. REV-ERB target genes involved in cholesterol and lipid metabolism are significantly**  
435 **downregulated by SR9009 treatment in a mouse model of NASH.** We analyzed several REV-ERB  
436 target genes (*Dhcr24*, *ApoE*, and *ApoC3*) by QPCR to determine expression level differences in the  
437 groups. As indicated by the graphs, all three target genes were significantly downregulated, suggesting  
438 that SR9009 treatment was suppressing these metabolic pathways but had poor efficacy for reducing  
439 steatosis.  
440

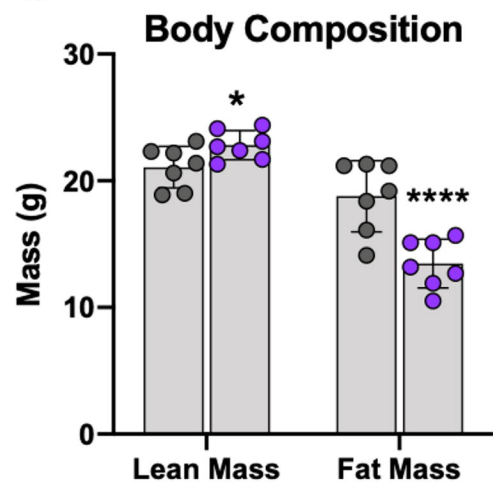
441 **S3 Fig. Whole liver section images showing Masson's Trichrome staining for fibrosis.** Scale bars  
442 indicate 1.56 mm.

443  
444 **S1 Table. Summary of Histo-Pathological Analysis on Liver Sections.**

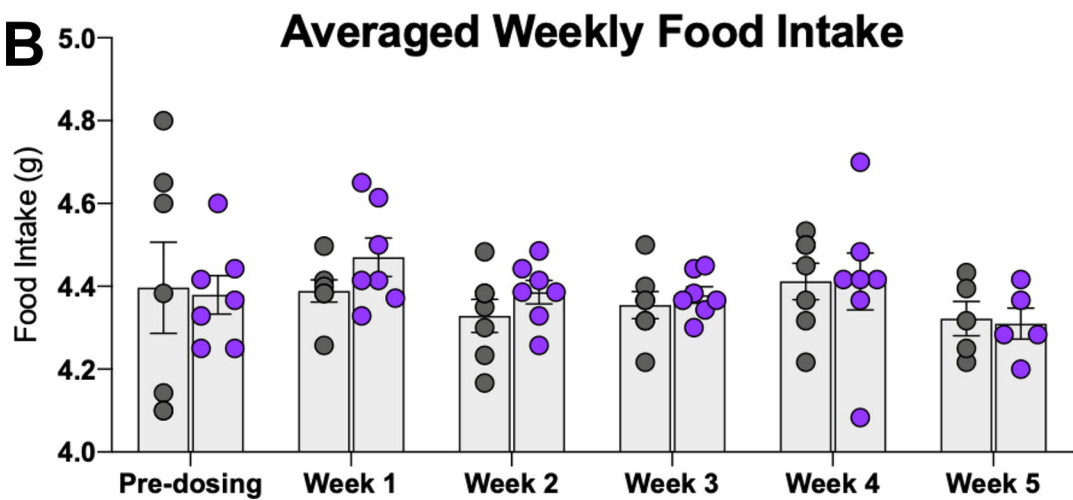
**A**



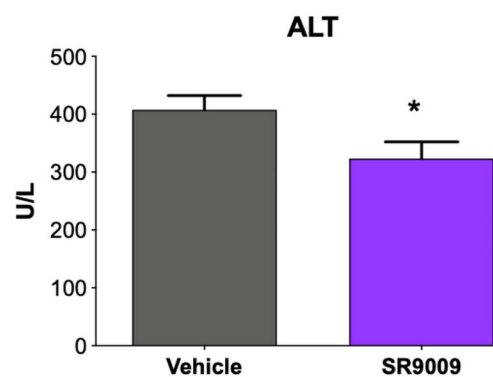
**C**



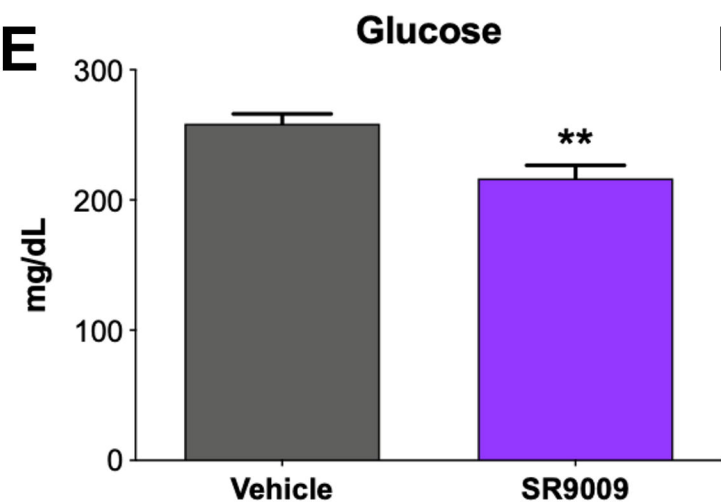
**B**



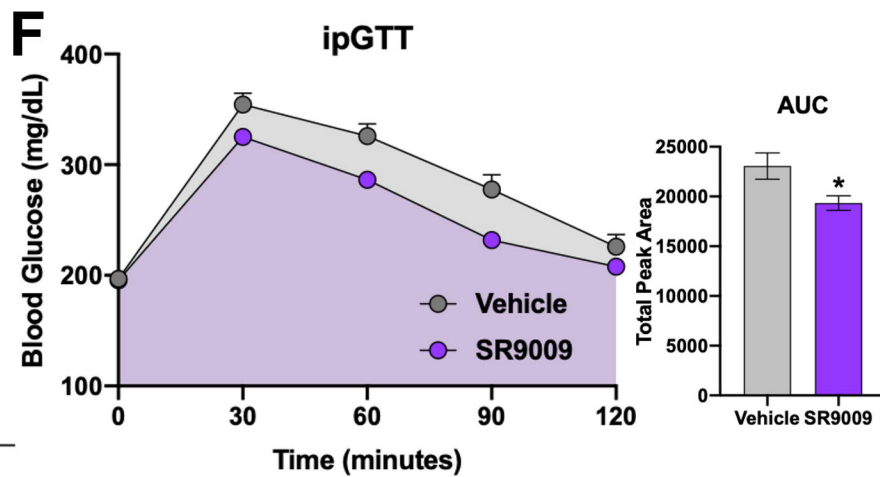
**D**



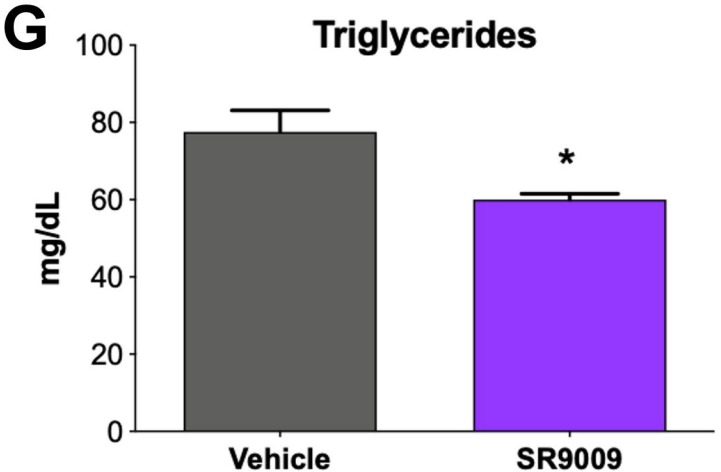
**E**



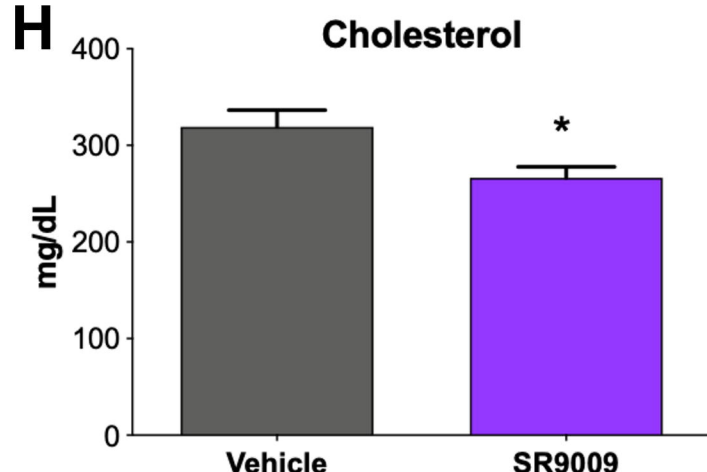
**F**



**G**

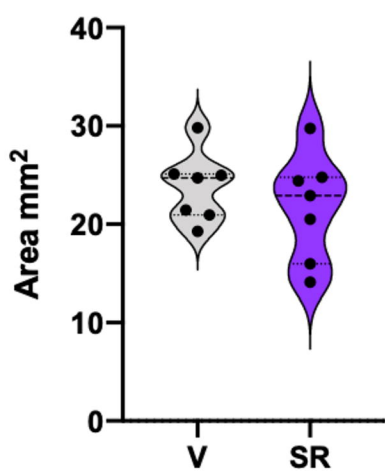


**H**

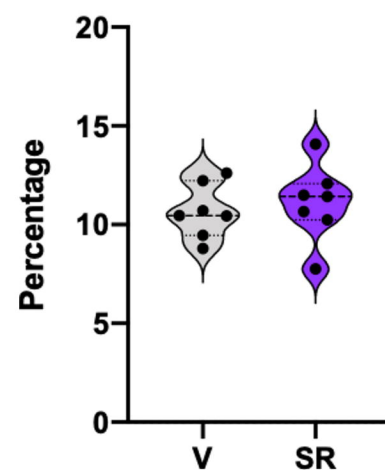




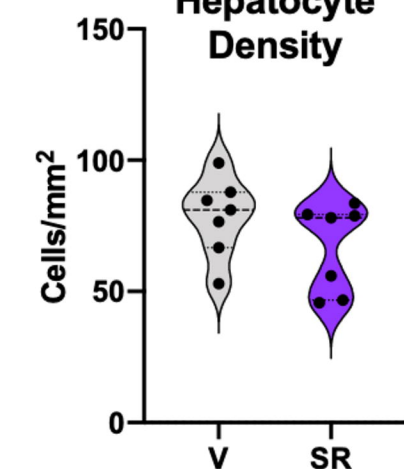
## A Total Lipid Area



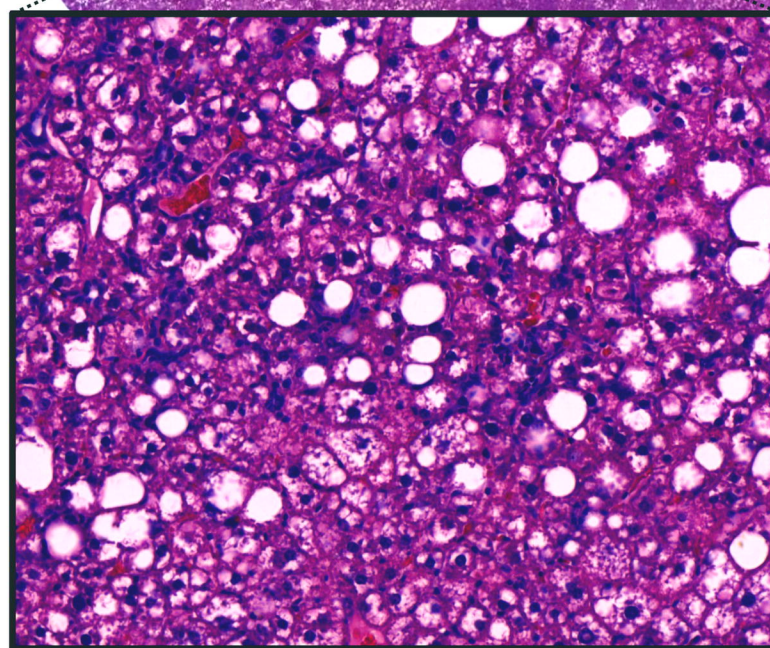
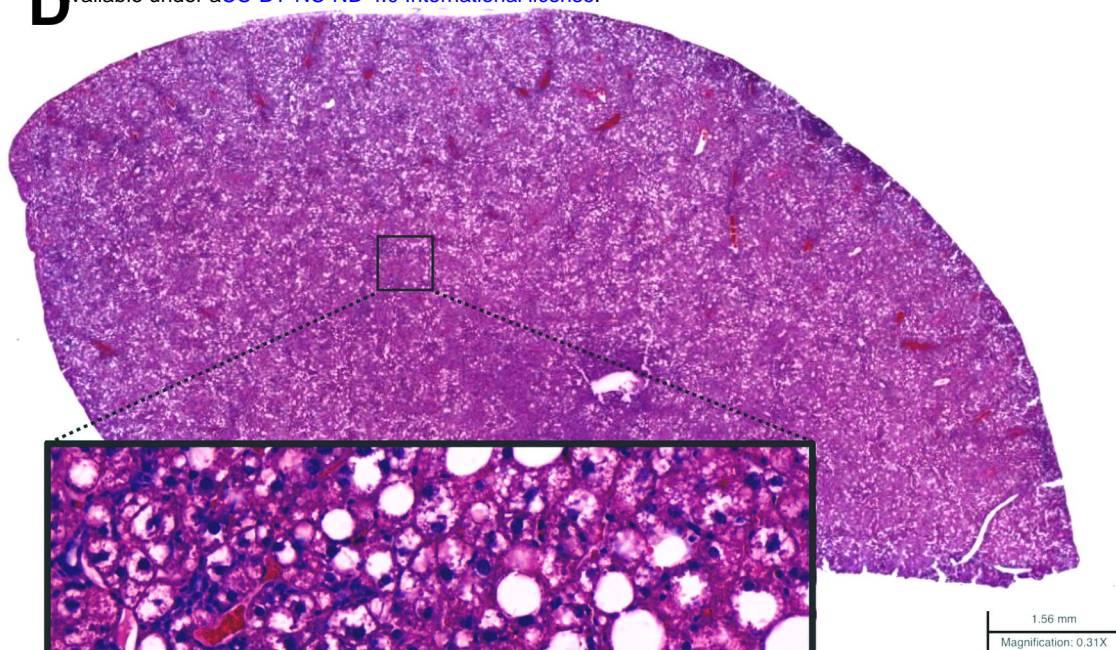
## B Lipid Area



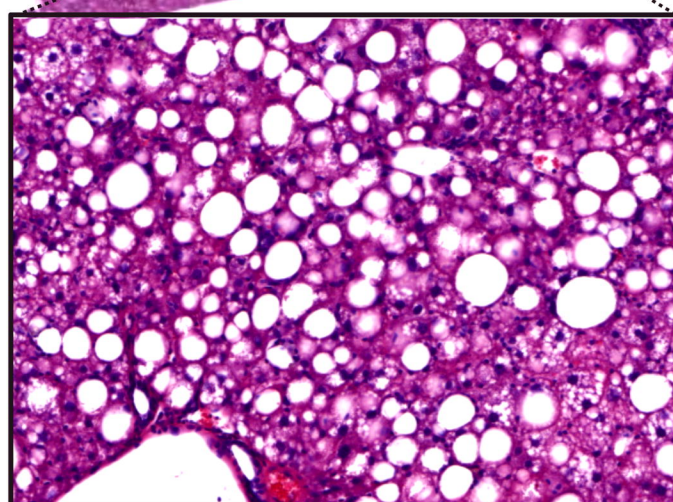
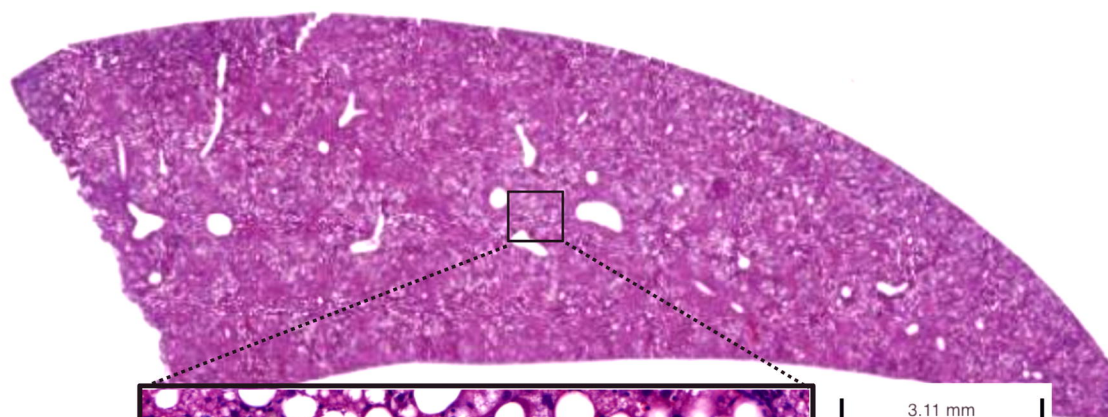
## C Ballooning Hepatocyte Density



## D



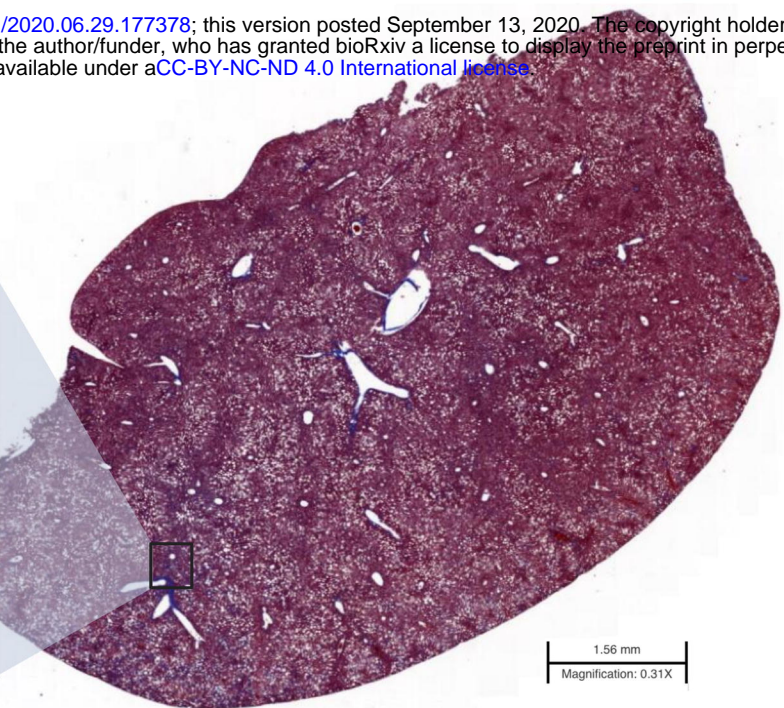
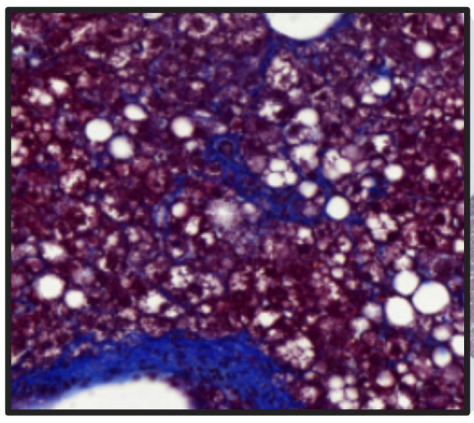
**Vehicle**



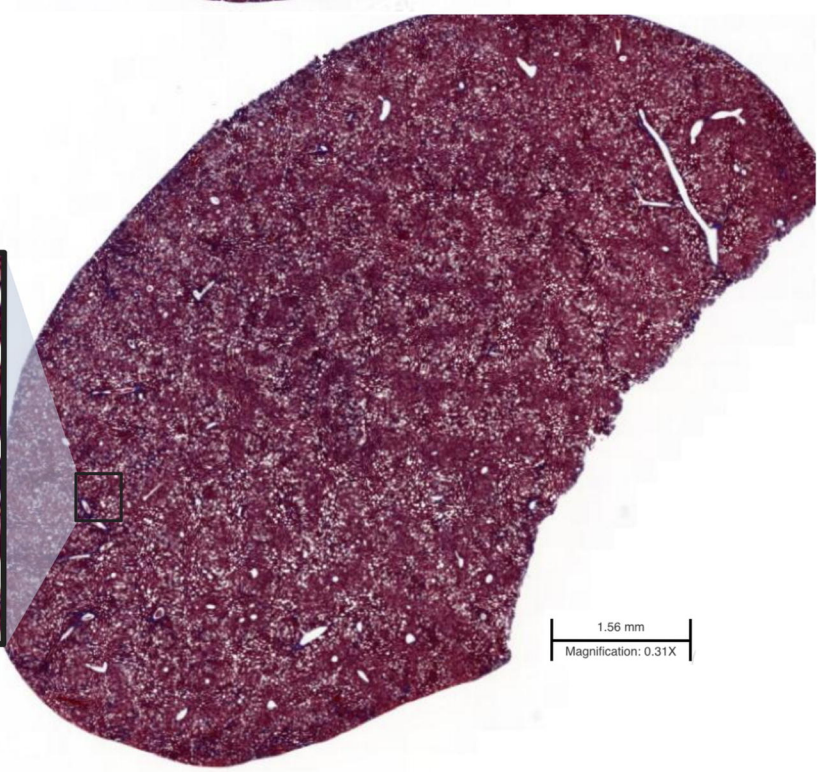
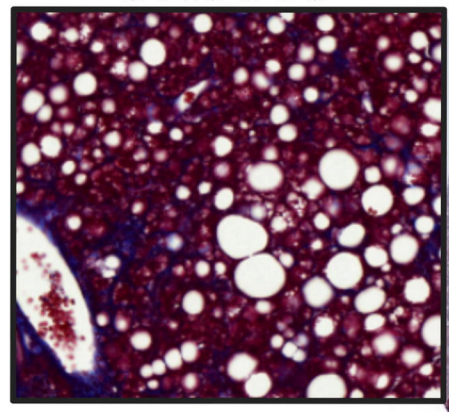
**SR9009**

**A**

**Vehicle**

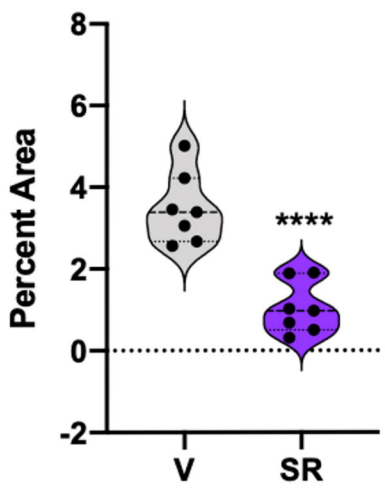


**SR9009**



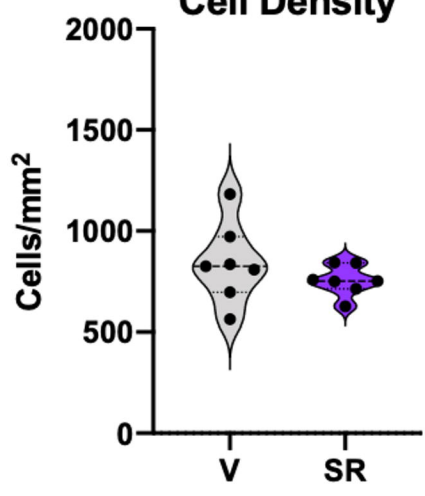
**B**

**Fibrosis**



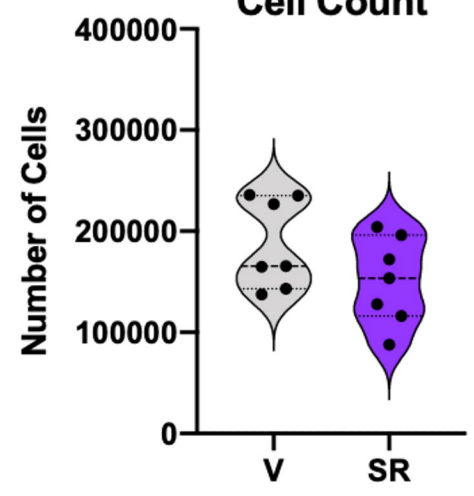
**C**

**Immune Cell Density**

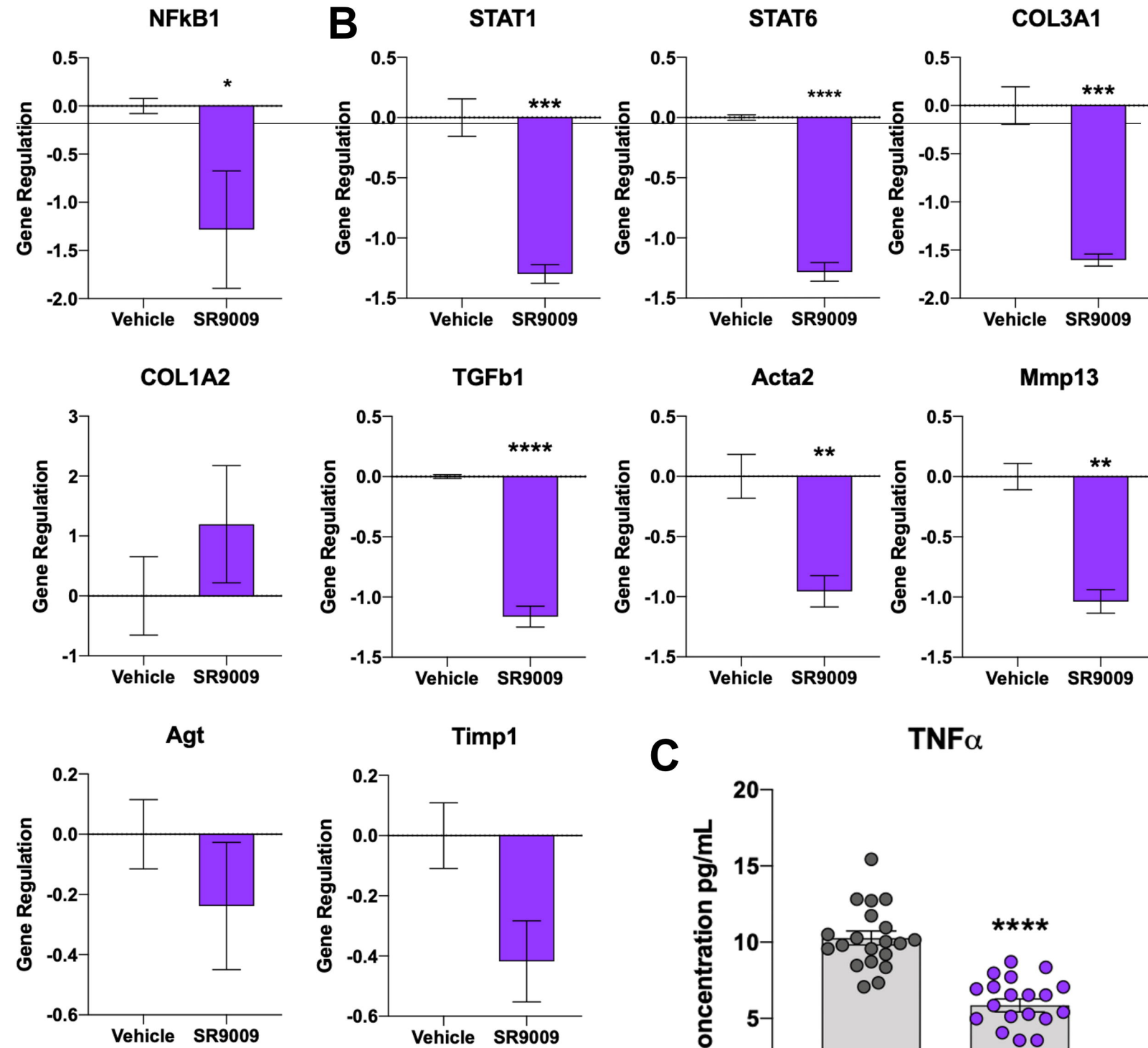
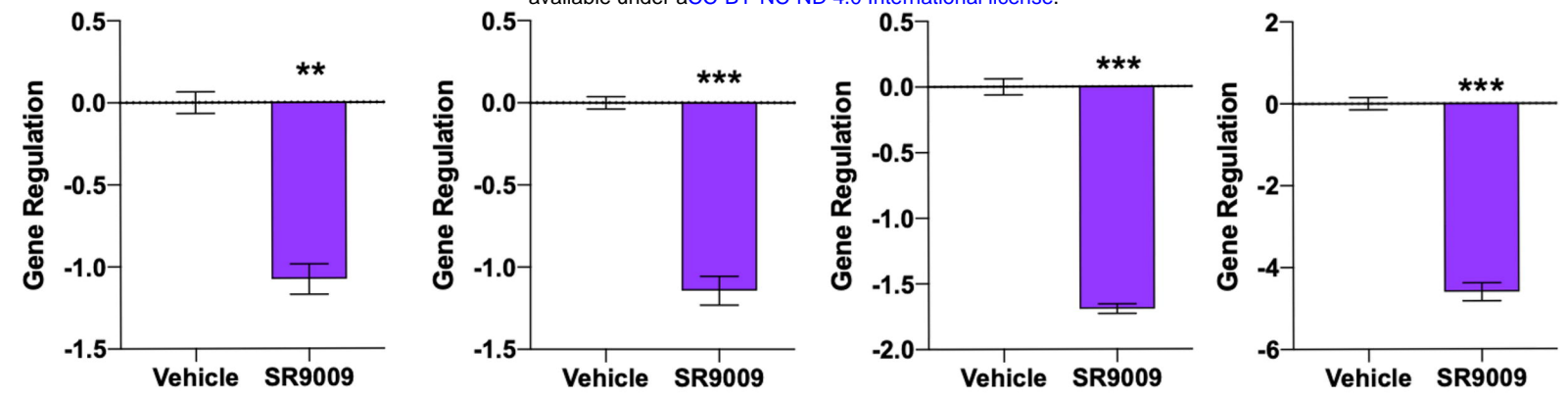


**D**

**Immune Cell Count**



**A**



**C**

